machines

MDPI

Article

Predictive Analysis of Crack Growth in Bearings via Neural Networks

Manpreet Singh [1,†], Dharma Teja Gopaluni [1,†], Sumit Shoor [1,†], Govind Vashishtha [2,3,*] and Sumika Chauhan [2]

[1] School of Mechanical Engineering, Lovely Professional University, Phagwara 144411, India; bainscoolbains@gmail.com (M.S.); gdt9804@gmail.com (D.T.G.); sumit.14602@gmail.com (S.S.)
[2] Faculty of Geoengineering, Mining and Geology, Wroclaw University of Science and Technology, Na Grobli 15, 50-421 Wroclaw, Poland; sumi.chauhan2@gmail.com
[3] Department of Mechanical Engineering, Graphic Era Deemed to be University, Dehradun 248002, India
* Correspondence: govindyudivashishtha@gmail.com
† This paper is an extended version of our paper published in International Conference on Production and Industrial Engineering, Jalandhar, India, 10–12 March 2023.

Abstract: Machine learning (ML) and artificial intelligence (AI) have emerged as the most advanced technologies today for solving issues as well as assessing and forecasting occurrences. The use of AI and ML in various organizations seeks to capitalize on the benefits of vast amounts of data based on scientific approaches, notably machine learning, which may identify patterns of decision-making and minimize the need for human intervention. The purpose of this research work is to develop a suitable neural network model, which is a component of AI and ML, to assess and forecast crack propagation in a bearing with a seeded crack. The bearing was continually run for many hours, and data were retrieved at time intervals that might be utilized to forecast crack growth. The variables root mean square (RMS), crest factor, signal-to-noise ratio (SNR), skewness, kurtosis, and Shannon entropy were collected from the continuously running bearing and utilized as input parameters, with the total crack area and crack width regarded as output parameters. Finally, utilizing several methodologies of the Neural Network tool in MATLAB, a realistic ANN model was trained to predict the crack area and crack width. It was observed that the ANN model performed admirably in predicting data with a better degree of accuracy. Through analysis, it was observed that the SNR was the most relevant parameter in anticipating data in bearing crack propagation, with an accuracy rate of 99.2% when evaluated as a single parameter, whereas in multiple parameter analysis, a combination of kurtosis and Shannon entropy gave a 99.39% accuracy rate.

Keywords: ANN; machine learning; bearing; crack propagation; statistical parameters

Citation: Singh, M.; Gopaluni, D.T.; Shoor, S.; Vashishtha, G.; Chauhan, S. Predictive Analysis of Crack Growth in Bearings via Neural Networks. *Machines* **2024**, *12*, 607. https://doi.org/10.3390/machines12090607

Academic Editor: Kai Cheng

Received: 29 July 2024
Revised: 26 August 2024
Accepted: 30 August 2024
Published: 1 September 2024

1. Introduction

Bearings, the unsung heroes of countless mechanical systems, are subjected to immense stresses and fatigue during operation [1,2]. These stresses can lead to the insidious growth of microscopic cracks, ultimately culminating in catastrophic failure. Understanding the intricate interplay between crack dimensions and propagation dynamics is crucial for ensuring the reliability and longevity of bearing systems [3–5].

This analysis delves into the complex world of crack propagation in bearings, aiming to shed light on the factors influencing crack growth and the crucial role of crack dimensions [6–8]. By meticulously examining the relationship between crack length, depth, and orientation with respect to the applied stresses and material properties, this study seeks to unveil the mechanisms governing crack evolution [9–11]. The findings of this investigation will hold significant implications. For instance, by accurately forecasting the rate of crack propagation, engineers can establish reliable estimations of bearing lifespan under varying operating conditions. Understanding the influence of crack dimensions on failure modes can guide the development of bearings with enhanced resistance to fatigue

and crack propagation [12,13]. The early detection and monitoring of crack dimensions can enable timely interventions, preventing catastrophic failures and ensuring safe operation [14,15]. Ren et al. [16] investigated the fracture behaviour of buried pipelines with corrosion defects subjected to seismic loads. Utilizing the extended finite element method, their study identified a critical crack tip angle near 5° in the corrosion area where maximum stress values occur. Xie et al. [17] delved into the complex influence of crack coupling on fatigue crack propagation in pipelines, moving beyond qualitative observations to provide a quantitative approach for predicting remaining useful life (RUL). Parsania et al. [18] investigated the complex interplay of multiple cracks in an infinite plate, focusing on the interaction between a main crack and an adjacent crack under various loading conditions. Utilizing the J-integral and finite element analysis, their study revealed that the presence of an adjacent crack can significantly influence the stress intensity factor (SIF) of the main crack, leading to intensifying, protective, or neutral effects depending on the relative position and orientation of the cracks.

This exploration into the realm of crack dimensions and their role in bearing failure will pave the way for a deeper comprehension of bearing behaviour, ultimately contributing to the design of more robust and reliable mechanical systems [19,20]. To address these issues, researchers have focussed on machine learning (ML) techniques, as they are more efficient, less costly, and more adaptable due to their involvement-free nature. In general, machine learning approaches are classified into supervised learning, unsupervised learning, semi-supervised learning, and reinforcement learning (RL) [21–23]. The artificial neural network (ANN) imitates the neurons of the human brain. The ANN architecture consists of input layers, hidden layers, and output layers.

In this work, a bearing with a seeded crack is taken and run continuously for several hours, with readings taken at regular intervals of time to determine the crack state. Furthermore, the measurements are trained and analyzed in MATLAB's neural network workspace to estimate the crack dimensions after properly training the system. The readings are obtained from the bearing while it is operating constantly, and these readings are taken with various combinations of the sets of inputs while retaining the outputs as total area and widths. These reading inputs and outputs are trained in the ANN model to test the accuracy of the prediction for a certain time period or reading.

The ANN model is developed in MATLAB, and the network type is a feed-forward back propagation neural network, since backpropagation is a learning approach that operates on a multilayer feed-forward neural network [24,25]. It continually learns a set of weights for predicting the class label. The training model is Levenberg–Marquardt optimization (TRAINLM). Furthermore, TRAINLM is a network training function that uses Levenberg–Marquardt optimization to update weight and bias variables [26,27]. Although it requires more memory than other algorithms, TRAINLM is frequently the fastest backpropagation method in the toolbox and is strongly recommended as a first-choice supervised technique [28,29].

Additionally, the LOGSIG transfer function is applied in the process, as A = logsig(N) takes a matrix of net input vectors, N, and returns the S-by-Q matrix, A, of the elements of N compressed into [0, 1] [30,31]. The LOGSIG function is a transfer function. Transfer functions compute the output of a layer based on its net input. This LOGSIG is used for the hidden layers and the PURELIN function is used for the output layer so that the regression graph will be linear and can measure the graph easily and accurately [32].

Various factors are used in the field of machine health monitoring and maintenance to analyze data obtained from machines in order to identify any irregularities or potential issues. The data obtained from a bearing with a seeded crack is analyzed in this work based on the parameters RMS, crest factor, SNR, skewness, kurtosis, and Shannon entropy. The parameters listed above are utilized to extract characteristics from data obtained from the bearing with the seeded crack that may be used to identify possible faults in the machine and anticipate crack growth.

The main contributions of this study are as follows:

- This research work successfully developed a practical artificial neural network (ANN) model capable of predicting crack area and width in a bearing with a seeded crack.
- The model utilizes key parameters like RMS, crest factor, SNR, skewness, kurtosis, and Shannon entropy, reflecting the practical application of these metrics in bearing condition monitoring.
- This study highlights the significant influence of SNR on predicting crack propagation when using it as a single input parameter.
- The combination of kurtosis and Shannon entropy achieved an even higher accuracy, demonstrating the potential for enhancing predictive performance through the integration of multiple parameters.
- This study validates the use of ANN models for predicting crack propagation in bearings, showcasing their ability to achieve high accuracy in real-world applications.

2. Research Methodology

2.1. Data Extraction

The bearing with the seeded crack was run continuously for several hours to extract some of the characteristics that may cause the crack to grow. A pictorial view of the seeded cracks at different hours is shown in Figure 1. RMS, crest factor, SNR, skewness, kurtosis, and Shannon entropy were the parameters which were analyzed to assess the propagation of cracks in the bearing. The data of these parameters are tabulated in Table 1.

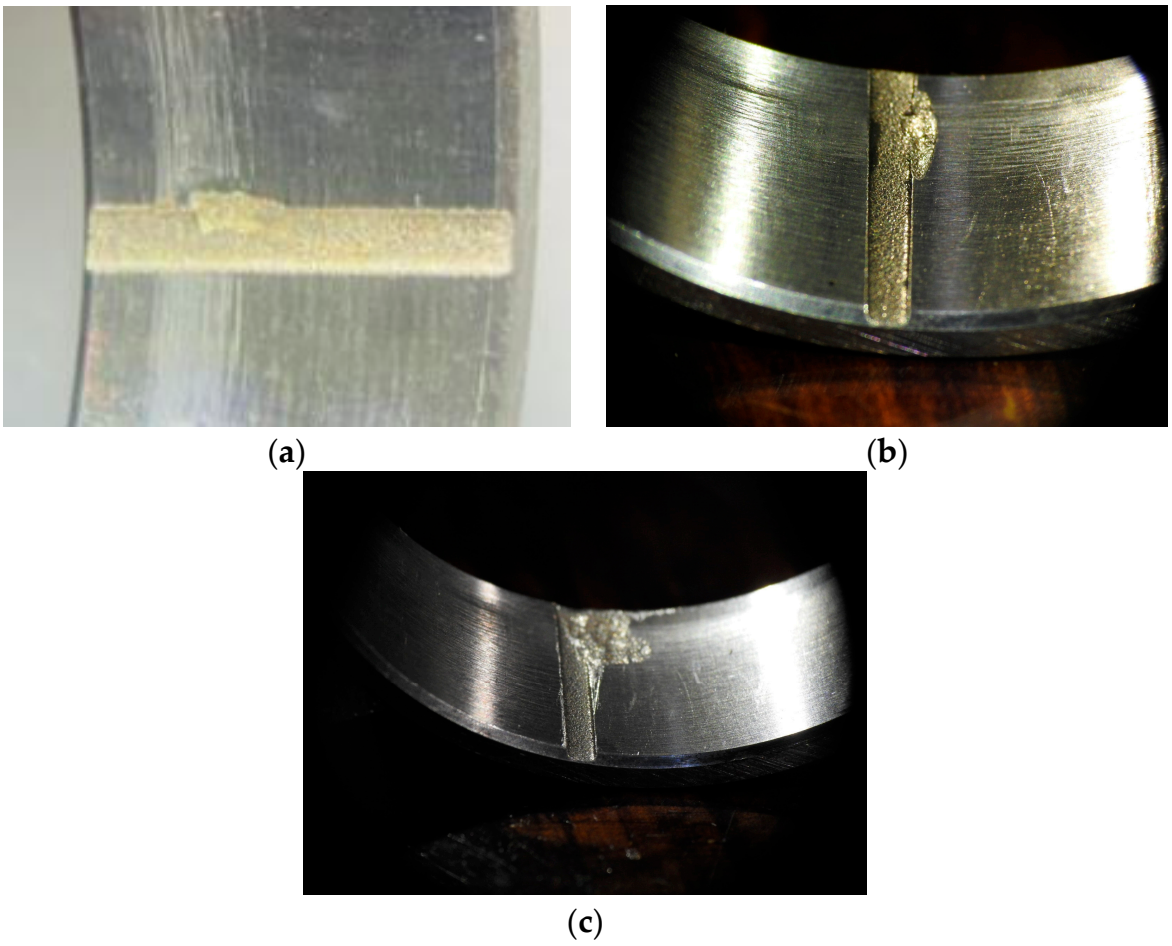

Figure 1. Pictorial view of cracks (**a**) at 90 h (**b**), at 192 h, and (**c**) at 285 h.

Table 1. Data retrieved from the bearing.

Time Duration in Hours	RMS (m/s^2)	Crest Factor	SNR	Skewness	Kurtosis	Shannon Entropy (10^7)	Input Variables	
							Total Area (mm^2)	Width (mm)
0	8.347	7.1256	22.98	0.189	5.554	2.42	24.86	1.82
10	10.22	6.8215	20.77	0.168	6.492	3.59	24.86	1.82
20	8.087	6.2457	22.33	0.208	5.527	2.02	24.86	1.82
30	8.472	8.0384	21.7	0.184	5.749	2.27	24.86	1.82
40	8.485	7.0794	22.46	0.22	5.626	2.27	24.86	1.82
50	8.448	8.2828	20.71	0.228	5.913	2.26	24.8625	1.82
60	8.456	7.3888	23.4	0.229	5.549	2.26	24.865	1.82
70	8.449	6.5549	20.99	0.223	5.618	2.25	24.8675	1.82
80	8.365	7.2492	23.45	0.223	5.542	2.19	24.96	1.82
90	8.308	6.418	22.34	0.221	5.603	2.17	24.96	1.8286
100	8.251	7.0285	21.54	0.216	5.752	2.13	24.96	1.8373
120	8.3	6.4237	22.2	0.218	5.679	2.16	25.36	1.895
140	8.601	6.7204	21.8	0.225	6.147	2.37	25.56	1.92
160	9.264	6.8881	20.35	0.168	5.521	2.8	26.0445	2.1
170	8.79	6.0588	20.29	0.18	5.728	2.48	26.4586	2.4766
180	7.68	13.357	23.6	0.119	8.537	2.03	26.978	3.1198
184	16.9	11.788	24.1	0.07	7.43	13.9	27.609	3.2798
188	8.1	14.3845	22.1	0.17	9.53	2.07	27.987	3.4399
192	7.97	11.439	22.9	0.04	7.67	1.98	28.275	3.6975
196	8.24	14.1009	24	0.11	11.6	2.19	28.345	4.0525
200	25.02	10.2382	19.67	0.129	7.312	30.7	28.778	4.867
204	22	9.5045	19.4	0.09	7.53	28	28.835	5.16
208	25.4	9.4644	22.4	0.11	7.15	20	28.892	5.4545
212	25.7	12.754	19.5	0.16	8.63	26	28.949	5.7482
216	24.9	8.8966	18.18	0.178	8.017	30.5	29.007	6.042
220	13.8	9.1122	24.3	0.12	7.09	7.27	28.885	7.0116
224	16	10.0815	21.2	0.16	7.63	15.2	28.945	7.0983
229	15.28	11.0412	23.31	0.078	8.1	10.2	29.15	7.231
232	19.2	11.2517	22.5	0.26	10.2	15.9	29.172	7.341
239	16.28	7.774	21.91	0.141	6.48	11.7	29.202	7.531
248	19.21	9.1612	17.67	0.151	6.135	12.2	29.324	7.761
259	14.86	7.3411	18.42	0.1707	6.824	9.58	29.556	8.631
267.5	8.723	9.1705	21.7	0.14	4.967	2.66	29.564	8.987
274.5	9.15	8.3301	19.51	0.041	6.653	3.06	31.019	9.362
278.5	9.178	9.6329	21.2	0.115	6.682	13.26	33.372	9.761
284.5	9.603	10.247	19.47	0.014	7.288	3.09	36.518	10.401
285	9.114	10.4396	19.35	0.009	7.954	2.74	40.157	10.967

2.2. Application of Neural Network

The data tabulated in Table 1 were imported into MATLAB 2021a and the proposed neural network model was trained. Keeping the time duration constant, the rest of the parameters were trained independently to see which factor was more affected by crack propagation by comparing the projected data output to the actual data [9,11–17].

Furthermore, the overall area and width of the crack were considered as the goal data. The ANN was trained using the TRAINLM algorithm for each parameter independently, and the expected output was simulated by feeding the algorithm sample data; the predicted total area and crack width were then compared to the actual data. The number of hidden layers was set to 10 when carrying out this study. The architecture used in this study is shown in Figure 2. This study was repeated for each parameter separately, and the ANN model with the lowest error in projected values was regarded to be the most influential factor in crack propagation.

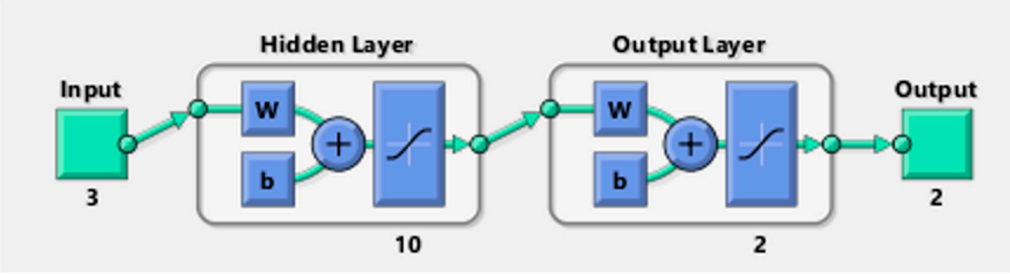

Figure 2. The architecture of NN used in the analysis.

Moreover, the method provides a regression plot for the input and output data, which establishes a regression line between two parameters and aids in the visualization of their linear correlations. The regression plot is commonly characterized as R, the plot that is formed comes with an R value, which stands for the regression value, and this value is regarded to be best and most accurate if R square equals 1 [10].

3. Results and Discussion

3.1. Single Parameters

Root Mean Square (RMS)

Using the RMS and time duration values as input parameters and the total area and breadth as targets, an ANN model was constructed, and values were forecasted using that model by providing some sample data as the input. Table 2 shows the projected values as well as the actual data.

Table 2. Analyzed data with the RMS as the input parameter.

Input Parameters		Actual/Target Values		Predicted Values		Accuracy (in %)
Time Duration	RMS (m/s^2)	Total Area (mm^2)	Width (mm)	Total Area (mm^2)	Width (mm)	
0	8.347	24.86	1.82	24.8600	1.82	100.0%
10	10.22	24.86	1.82	24.8600	1.82	100.0%
20	8.087	24.86	1.82	24.8600	1.82	100.0%
30	8.472	24.86	1.82	24.8600	1.82	100.0%
40	8.485	24.86	1.82	24.8600	1.82	100.0%
50	8.448	24.8625	1.82	24.8601	1.82	100.0%
60	8.456	24.865	1.82	24.8604	1.82	100.0%
70	8.449	24.8675	1.82	24.8619	1.8200	100.0%
80	8.365	24.96	1.82	24.8708	1.8200	99.8%
90	8.308	24.96	1.8286	24.9076	1.8202	99.7%
100	8.251	24.96	1.8373	25.0026	1.8249	99.6%
120	8.3	25.36	1.8953	25.3488	1.8787	99.5%
140	8.601	25.56	1.92	25.5771	1.9401	99.4%
160	9.264	26.0445	2.1	26.0410	2.0878	99.7%
170	8.79	26.4586	2.4766	26.2826	2.4391	98.9%
180	7.68	26.978	3.1198	27.6182	3.0798	98.2%
184	16.9	27.609	3.2798	24.8600	3.2777	94.4%
188	8.1	27.987	3.4399	27.9953	3.4596	99.7%
192	7.97	28.275	3.6975	28.2749	3.6800	99.8%
196	8.24	28.345	4.0525	28.1086	3.8432	96.9%
200	25.02	28.778	4.867	24.86	4.8627	92.1%
204	22	28.83525	5.16	24.86	5.1546	92.0%
208	25.4	28.8925	5.4545	24.86	5.4346	91.7%
212	25.7	28.94975	5.7482	24.86	5.7407	91.7%
216	24.9	29.007	6.042	24.86	6.0431	91.6%
220	13.8	28.885	7.0116	24.86	6.8938	91.1%
224	16	28.945	7.0983	24.86	7.0906	91.7%
229	15.28	29.15	7.231	24.86	7.2384	91.3%
232	19.2	29.1725	7.341	24.86	7.5194	90.1%
239	16.28	29.202	7.531	24.86	7.4396	90.7%
248	19.21	29.324	7.761	24.86	7.7607	91.0%
259	14.86	29.556	8.631	24.86	8.6296	90.5%
267.5	8.723	29.564	8.987	24.86	8.9862	90.5%
274.5	9.15	31.019	9.362	24.86	9.2226	86.9%
278.5	9.178	33.372	9.761	24.86	9.7644	82.9%
284.5	9.603	36.518	10.401	24.86	10.3986	76.5%
285	9.114	40.157	10.967	24.86	10.9600	69.2%

The predicted values were created using the ANN model, and the accuracy of the trained model was calculated using the actual values. The trained model's accuracy was

calculated by taking the average of all the values. The findings indicate that RMS as a single parameter had an accuracy of 94.2%. The accuracy was computed using the formula below [10].

$$\text{Accuracy} = 1 - (\text{Predicted value} - \text{Actual value})/\text{Predicted value} \quad (1)$$

The ANN model was built with the crest factor and time duration values as input parameters and the total area and breadth as targets, and values were projected using this model by supplying some sample data as the input. Table 3 displays both the predicted and actual numbers.

Table 3. Analyzed data with the crest factor as input parameter.

Input Parameters		Actual/Target Values		Predicted Values		Accuracy (in %)
Time Duration	Crest Factor	Total Area (mm^2)	Width (mm)	Total Area (mm^2)	Width (mm)	
0	7.1256	24.86	1.82	24.8600	1.82	100.0%
10	6.8215	24.86	1.82	24.8600	1.82	100.0%
20	6.2457	24.86	1.82	24.8600	1.82	100.0%
30	8.0384	24.86	1.82	24.8600	1.82	100.0%
40	7.0794	24.86	1.82	24.8600	1.82	100.0%
50	8.2828	24.8625	1.82	24.8600	1.82	100.0%
60	7.3888	24.865	1.82	24.8600	1.82	100.0%
70	6.5549	24.8675	1.82	24.8600	1.8200	100.0%
80	7.2492	24.96	1.82	24.8600	1.8200	99.8%
90	6.418	24.96	1.8286	25.6415	1.8200	98.4%
100	7.0285	24.96	1.8373	24.9593	1.8200	99.5%
120	6.4237	25.36	1.8953	25.7792	1.8200	97.1%
140	6.7204	25.56	1.92	25.8987	1.8200	96.6%
160	6.8881	26.0445	2.1	26.0445	1.8200	92.3%
170	6.0588	26.4586	2.4766	26.4577	1.8200	82.0%
180	13.357	26.978	3.1198	24.8600	3.1218	95.7%
184	11.788	27.609	3.2798	24.8600	3.2773	94.4%
188	14.3845	27.987	3.4399	24.8600	3.3777	92.8%
192	11.439	28.275	3.6975	24.8600	3.6949	93.1%
196	14.1009	28.345	4.0525	24.8600	4.0541	93.0%
200	10.2382	28.778	4.867	28.7983074	4.9050	99.6%
204	9.5045	28.83525	5.16	28.85434946	5.1448	99.8%
208	9.4644	28.8925	5.4545	28.89521537	5.4927	99.6%
212	12.754	28.94975	5.7482	24.86	5.7404	91.7%
216	8.8966	29.007	6.042	28.96290978	6.0790	99.6%
220	9.1122	28.885	7.0116	29.00115216	6.4209	95.2%
224	10.0815	28.945	7.0983	29.04998962	6.8310	97.9%
229	11.0412	29.15	7.231	29.10491902	7.2469	99.8%
232	11.2517	29.1725	7.341	29.12729376	7.4323	99.3%
239	7.774	29.202	7.531	29.18287349	7.5263	99.9%
248	9.1612	29.324	7.761	29.20599516	8.0095	98.2%
259	7.3411	29.556	8.631	29.5600133	8.6280	100.0%
267.5	9.1705	29.564	8.987	29.69694264	8.7809	98.6%
274.5	8.3301	31.019	9.362	31.01305386	9.3511	99.9%
278.5	9.6329	33.372	9.761	32.19229614	9.7187	98.0%
284.5	10.247	36.518	10.401	36.50258921	10.4959	99.5%
285	10.4396	40.157	10.967	36.82257261	10.5398	93.4%

By repeating the accuracy calculation method from the previous stage, the crest factor exhibited 97.4% accuracy. The same procedure was followed for the remaining parameters, namely SNR, skewness, kurtosis, and Shannon entropy, and the predicted data, as well as

the actual data's accuracy, are shown in Table 4. The regression graphs for all the parameters were also obtained through ANN, as shown in Figures 3–8.

Table 4. Accuracy percentage of remaining parameters.

S. No.	Input Parameters	Accuracy (in %)
1	SNR	99.2
2	Skewness	98.6
3	Kurtosis	97.1
4	Shannon entropy (10^7)	97.8

It can be observed from Table 4 that the SNR was 99.2%, skewness was 98.6%, kurtosis was 97.1%, and Shannon entropy was 97.8% accurate. Furthermore, the analysis is carried out by conducting various permutations and combinations of the input parameters. In this study, the number of input parameters was reduced to three, with the time duration staying constant while the other parameters were shuffled in various combinations.

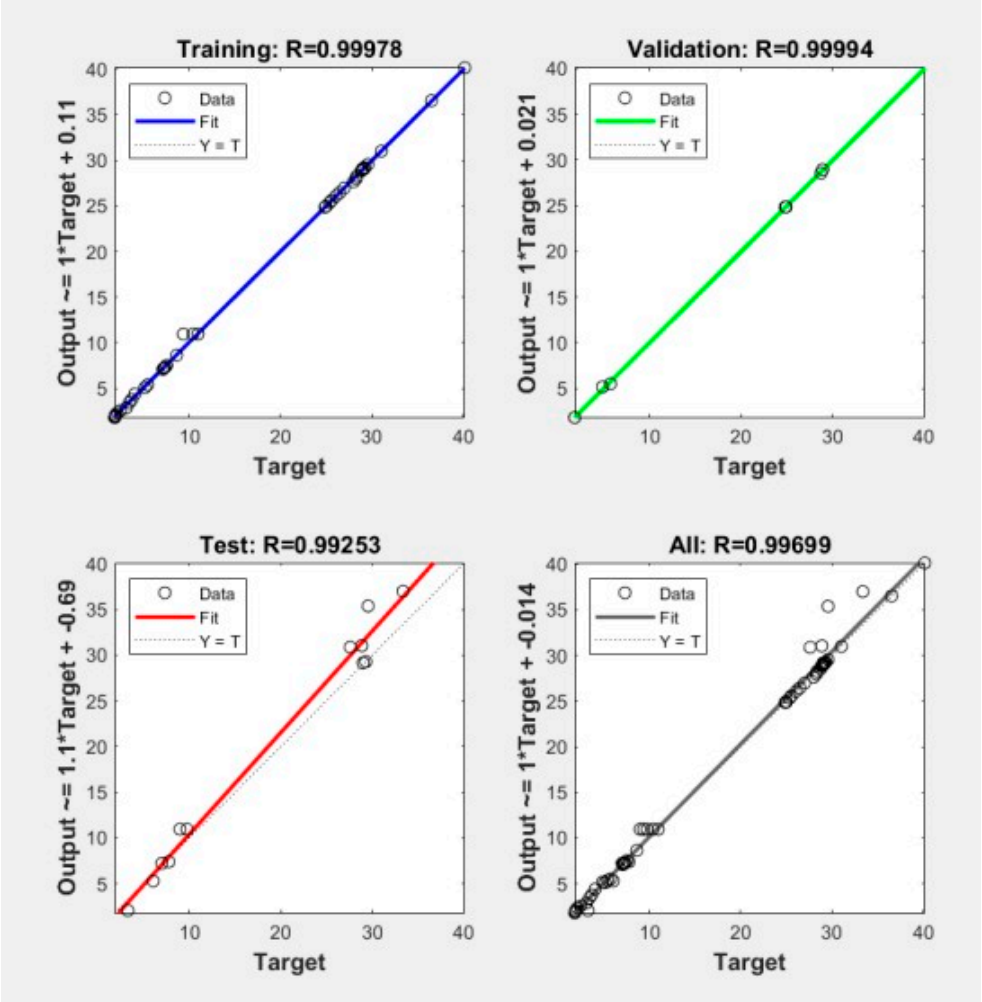

Figure 3. Regression plot for the RMS.

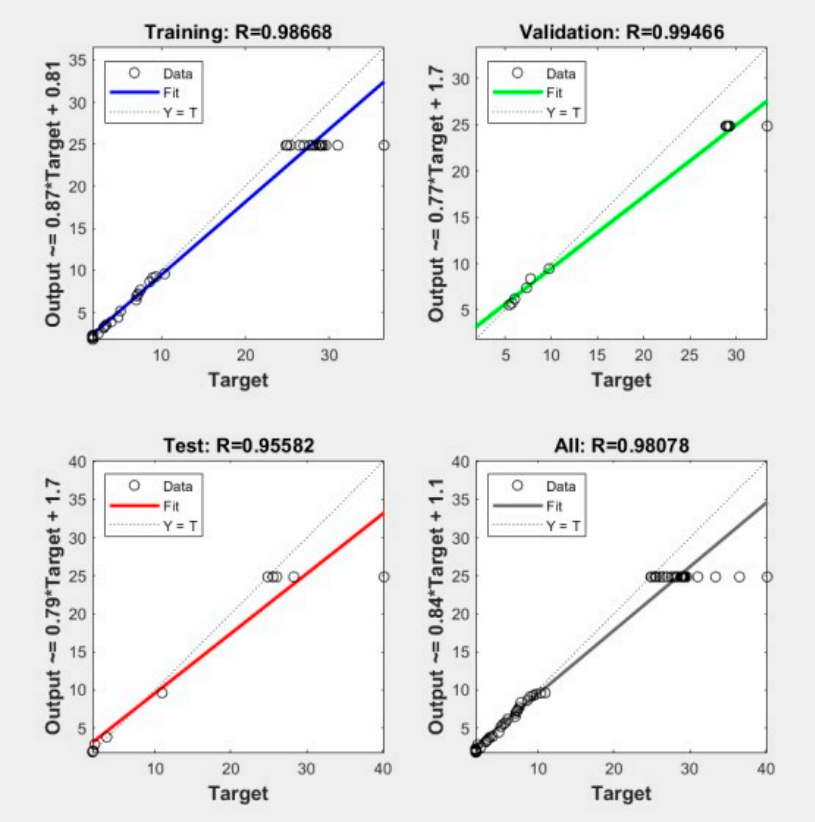

Figure 4. Regression plot for the crest factor.

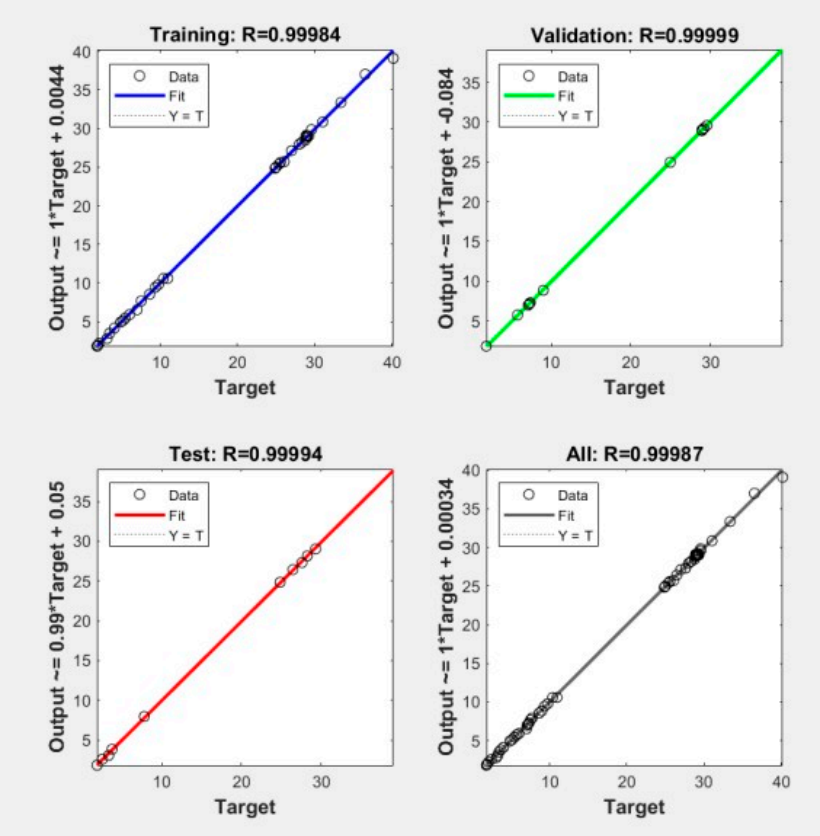

Figure 5. Regression plot for the SNR.

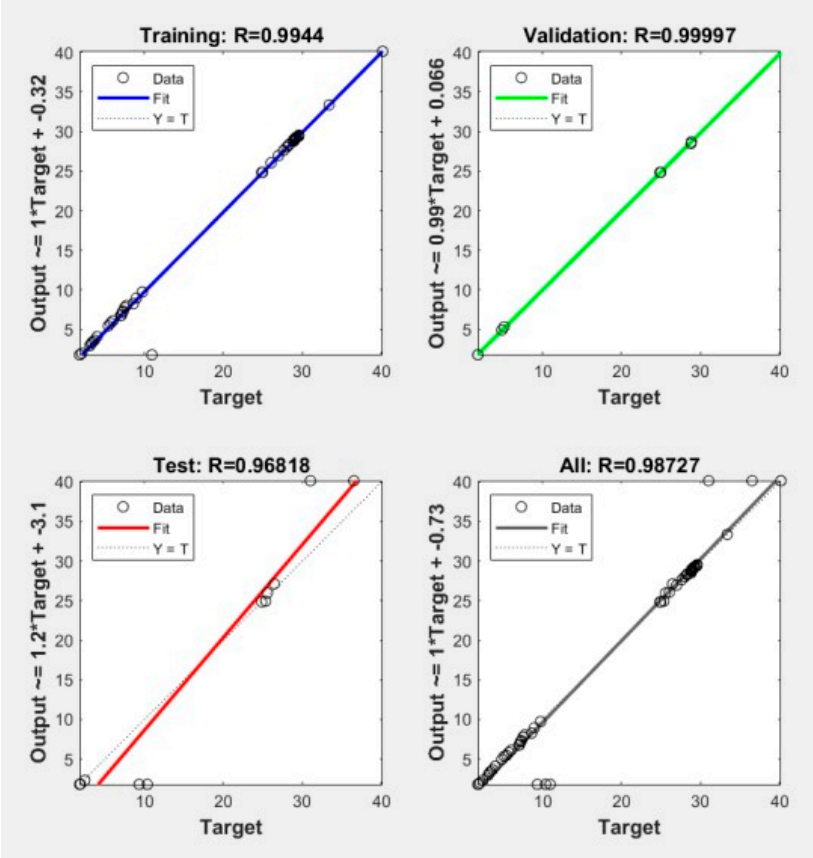

Figure 6. Regression plot for skewness.

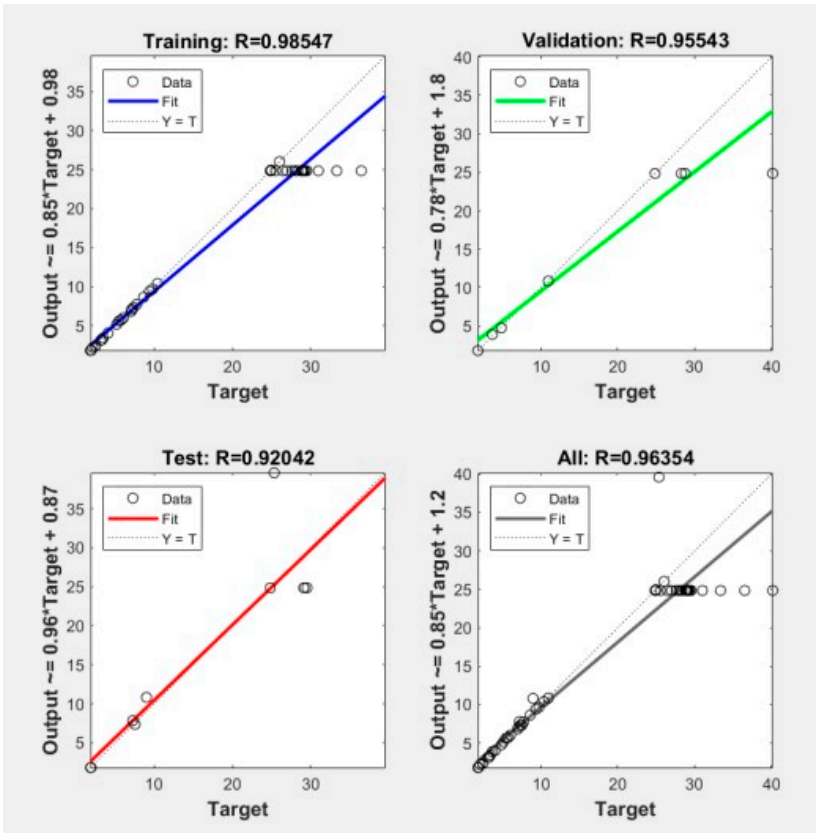

Figure 7. Regression plot for kurtosis.

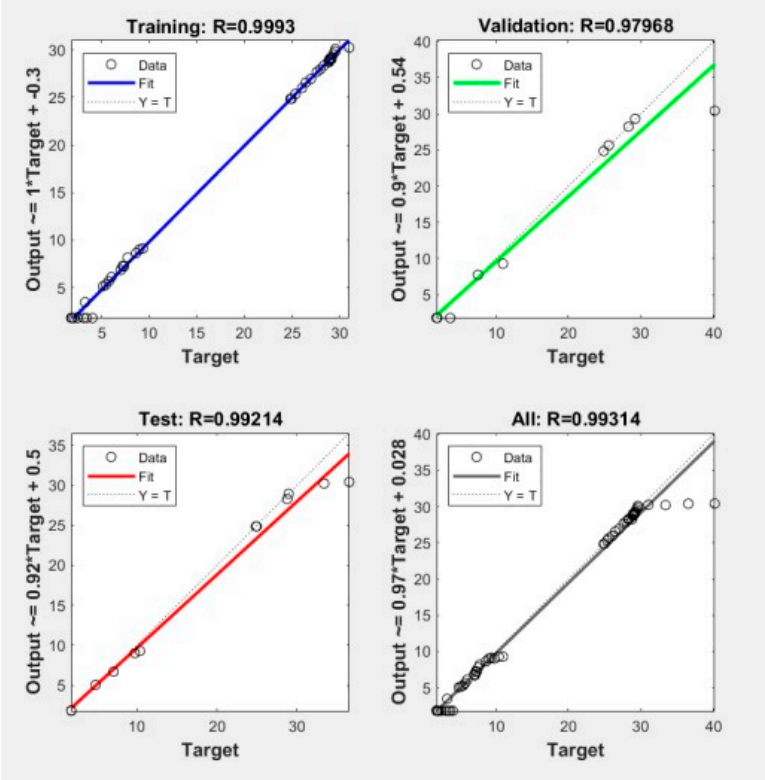

Figure 8. Regression plot for Shannon entropy.

3.2. Multiple Parameters

To validate the efficacy of the proposed method, the analysis of multiple parameters was also carried out.

3.2.1. RMS and Crest Factor

An ANN model was built with the RMS, crest factor, and time duration values as input parameters and the total area and breadth as targets, and values were projected using that model by supplying some sample data as the input. Table 5 displays both the predicted and actual numbers.

Table 5. Analyzed data with the RMS and crest factor as input parameters.

Input Parameters			Actual/Target Values		Predicted Values		Accuracy (in %)
Time Duration	RMS (m/s^2)	Crest Factor	Total Area (mm^2)	Width (mm)	Total Area (mm^2)	Width (mm)	
0	8.347	7.1256	7.1256	24.86	1.82	24.862	99.99%
10	10.22	6.8215	6.8215	24.86	1.82	24.860	100.00%
20	8.087	6.2457	6.2457	24.86	1.82	24.865	99.98%
30	8.472	8.0384	8.0384	24.86	1.82	24.869	99.97%
40	8.485	7.0794	7.0794	24.86	1.82	24.875	99.94%
50	8.448	8.2828	8.2828	24.8625	1.82	24.886	99.91%
60	8.456	7.3888	7.3888	24.865	1.82	24.904	99.84%
70	8.449	6.5549	6.5549	24.8675	1.82	24.934	99.73%
80	8.365	7.2492	7.2492	24.96	1.82	24.981	99.92%
90	8.308	6.418	6.418	24.96	1.8286	25.051	99.64%
100	8.251	7.0285	7.0285	24.96	1.8373	25.151	99.24%
120	8.3	6.4237	6.4237	25.36	1.8953	25.468	99.58%

Table 5. *Cont.*

Input Parameters			Actual/Target Values		Predicted Values		Accuracy (in %)
Time Duration	RMS (m/s^2)	Crest Factor	Total Area (mm^2)	Width (mm)	Total Area (mm^2)	Width (mm)	
140	8.601	6.7204	6.7204	25.56	1.92	25.940	98.54%
160	9.264	6.8881	6.8881	26.0445	2.1	25.753	98.87%
170	8.79	6.0588	6.0588	26.4586	2.4766	26.869	98.47%
180	7.68	13.357	13.357	26.978	3.1198	27.475	98.19%
184	16.9	11.788	11.788	27.609	3.2798	27.437	99.37%
188	8.1	14.3845	14.3845	27.987	3.4399	27.872	99.59%
192	7.97	11.439	11.439	28.275	3.6975	27.986	98.97%
196	8.24	14.1009	14.1009	28.345	4.0525	28.436	99.68%
200	25.02	10.2382	10.2382	28.778	4.867	28.752	99.91%
204	22	9.5045	9.5045	28.83525	5.16	28.785	99.83%
208	25.4	9.4644	9.4644	28.8925	5.4545	28.897	99.98%
212	25.7	12.754	12.754	28.94975	5.7482	28.929	99.93%
216	24.9	8.8966	8.8966	29.007	6.042	28.099	96.77%
220	13.8	9.1122	9.1122	28.885	7.0116	28.900	99.95%
224	16	10.0815	10.0815	28.945	7.0983	29.036	99.69%
229	15.28	11.0412	11.0412	29.15	7.231	29.220	99.76%
232	19.2	11.2517	11.2517	29.1725	7.341	29.294	99.59%
239	16.28	7.774	7.774	29.202	7.531	29.131	99.76%
248	19.21	9.1612	9.1612	29.324	7.761	29.343	99.93%
259	14.86	7.3411	7.3411	29.556	8.631	29.516	99.87%
267.5	8.723	9.1705	9.1705	29.564	8.987	30.492	96.96%
274.5	9.15	8.3301	8.3301	31.019	9.362	29.425	94.58%
278.5	9.178	9.6329	9.6329	33.372	9.761	33.380	99.98%
284.5	9.603	10.247	10.247	36.518	10.401	35.734	97.81%
285	9.114	10.4396	10.4396	40.157	10.967	38.663	96.14%

It can be observed from Table 5 that the RMS and crest factor showed 99.18% accuracy on average. The regression plot obtained through ANN and the performance curve are also shown in Figures 9 and 10, respectively.

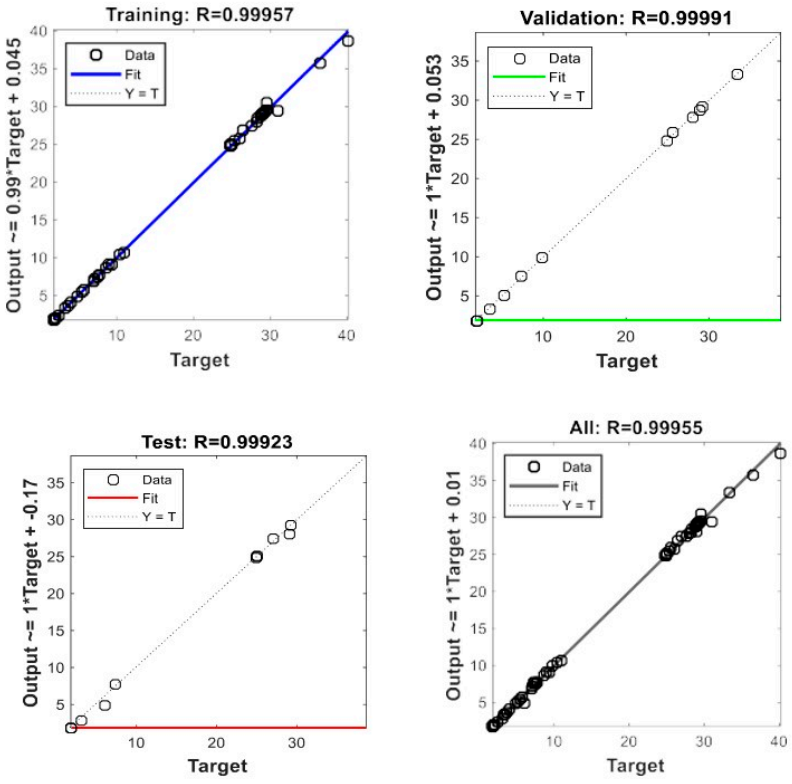

Figure 9. Regression plot for the RMS and crest factor.

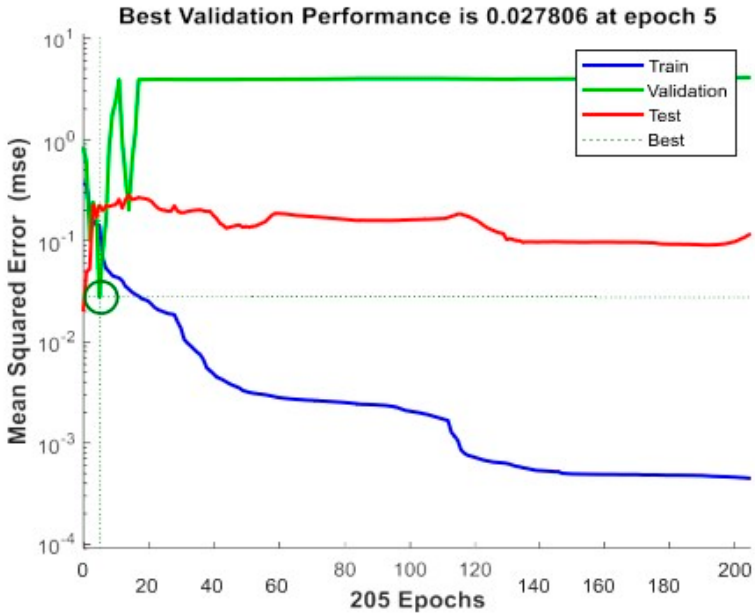

Figure 10. Performance plot for the RMS and crest factor.

3.2.2. RMS and SNR

In another case, the RMS, SNR, and time duration values were taken as input parameters and the total area and breadth were considered as research goals. An ANN model was developed, and values were projected using that model by feeding some sample data as the input. Table 6 shows both the expected and actual results.

Table 6. Analyzed data with the RMS and SNR as input parameters.

Input Parameters			Actual/Target Values		Predicted Values		Accuracy (in %)
Time Duration	RMS (m/s^2)	SNR	Total Area (mm^2)	Width (mm)	Total Area (mm^2)	Width (mm)	
0	8.347	22.98	22.98	24.86	1.82	24.860	100.00%
10	10.22	20.77	20.77	24.86	1.82	24.860	100.00%
20	8.087	22.33	22.33	24.86	1.82	24.860	100.00%
30	8.472	21.7	21.7	24.86	1.82	24.860	100.00%
40	8.485	22.46	22.46	24.86	1.82	24.860	100.00%
50	8.448	20.71	20.71	24.8625	1.82	24.860	99.99%
60	8.456	23.4	23.4	24.865	1.82	24.860	99.98%
70	8.449	20.99	20.99	24.8675	1.82	24.860	99.97%
80	8.365	23.45	23.45	24.96	1.82	24.963	99.99%
90	8.308	22.34	22.34	24.96	1.8286	24.861	99.60%
100	8.251	21.54	21.54	24.96	1.8373	24.860	99.60%
120	8.3	22.2	22.2	25.36	1.8953	25.359	100.00%
140	8.601	21.8	21.8	25.56	1.92	25.950	98.50%
160	9.264	20.35	20.35	26.0445	2.1	26.044	100.00%
170	8.79	20.29	20.29	26.4586	2.4766	26.459	100.00%
180	7.68	23.6	23.6	26.978	3.1198	27.960	96.49%
184	16.9	24.1	24.1	27.609	3.2798	27.608	100.00%
188	8.1	22.1	22.1	27.987	3.4399	27.987	100.00%
192	7.97	22.9	22.9	28.275	3.6975	28.120	99.45%
196	8.24	24	24	28.345	4.0525	28.344	100.00%
200	25.02	19.67	19.67	28.778	4.867	24.860	84.24%
204	22	19.4	19.4	28.83525	5.16	24.860	84.01%
208	25.4	22.4	22.4	28.8925	5.4545	28.892	100.00%
212	25.7	19.5	19.5	28.94975	5.7482	24.860	83.55%
216	24.9	18.18	18.18	29.007	6.042	24.860	83.32%

Table 6. *Cont.*

Input Parameters			Actual/Target Values		Predicted Values		Accuracy (in %)
Time Duration	RMS (m/s^2)	SNR	Total Area (mm^2)	Width (mm)	Total Area (mm^2)	Width (mm)	
220	13.8	24.3	24.3	28.885	7.0116	25.148	85.14%
224	16	21.2	21.2	28.945	7.0983	31.529	91.80%
229	15.28	23.31	23.31	29.15	7.231	29.149	100.00%
232	19.2	22.5	22.5	29.1725	7.341	29.172	100.00%
239	16.28	21.91	21.91	29.202	7.531	29.569	98.76%
248	19.21	17.67	17.67	29.324	7.761	24.860	82.04%
259	14.86	18.42	18.42	29.556	8.631	33.783	87.49%
267.5	8.723	21.7	21.7	29.564	8.987	27.384	92.04%
274.5	9.15	19.51	19.51	31.019	9.362	31.018	100.00%
278.5	9.178	21.2	21.2	33.372	9.761	28.197	81.65%
284.5	9.603	19.47	19.47	36.518	10.401	36.518	100.00%
285	9.114	19.35	19.35	40.157	10.967	31.544	72.69%

It can be observed from Table 6 that the RMS and SNR showed 95.14% accuracy on average. The regression plot and the performance plot of this analysis are shown in Figures 11 and 12.

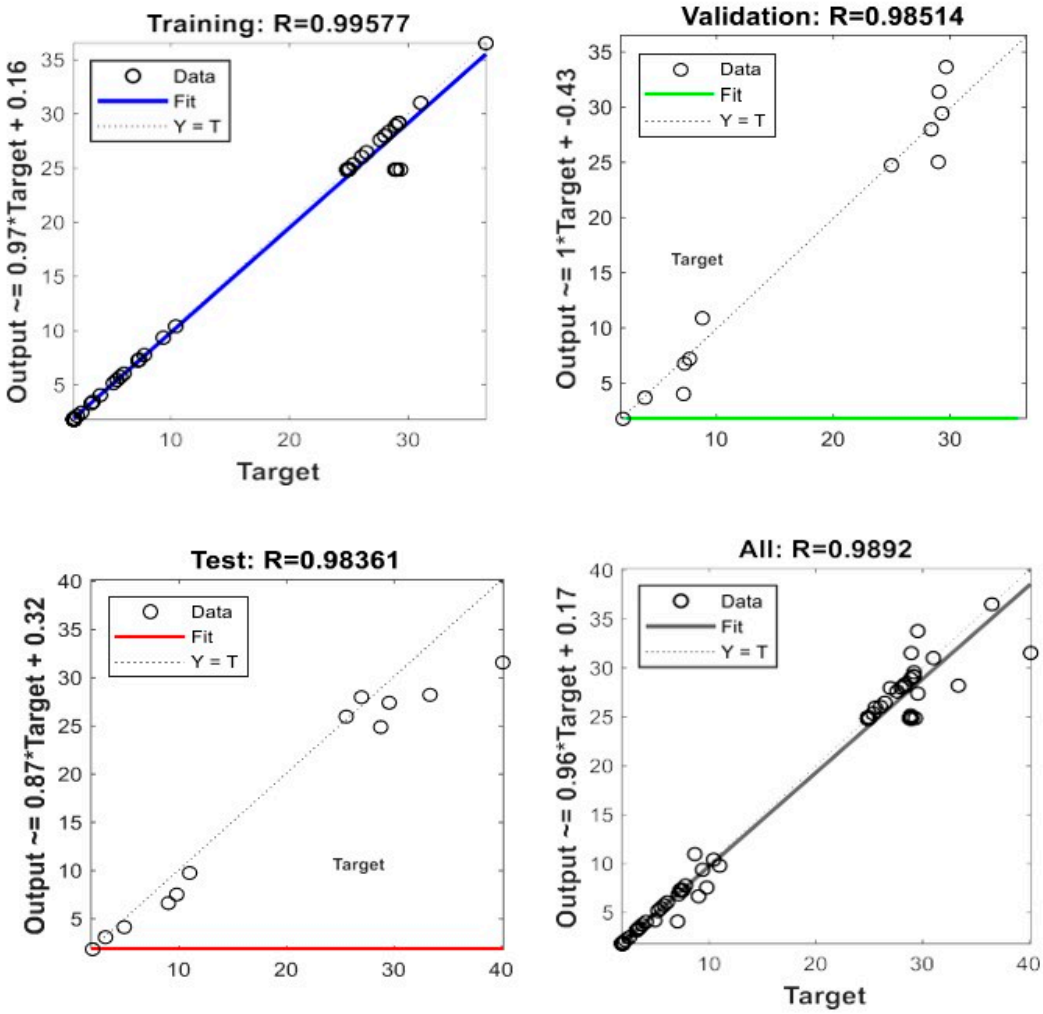

Figure 11. Regression plot for the RMS and SNR.

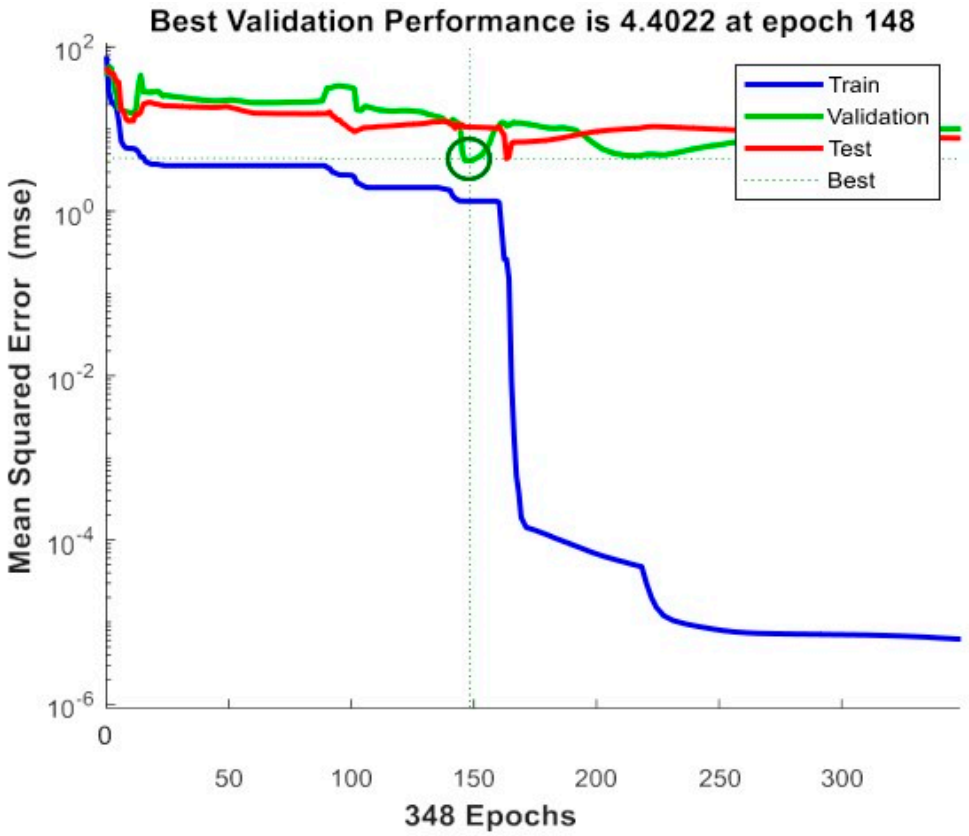

Figure 12. Performance plot for the RMS and SNR.

3.2.3. RMS and Skewness

An ANN model was constructed with the RMS, skewness, and time duration values as input parameters and the total area and breadth as targets, and values were projected using this model by feeding it some sample data. Table 7 displays both the predicted and actual outcomes.

Table 7. Analyzed data with the RMS and skewness as input parameters.

Input Parameters			Actual/Target Values		Predicted Values		Accuracy (in %)
Time Duration	RMS (m/s^2)	Skewness	Total Area (mm^2)	Width (mm)	Total Area (mm^2)	Width (mm)	
0	8.347	0.189	0.189	24.86	1.82	24.890	99.88%
10	10.22	0.168	0.168	24.86	1.82	24.911	99.80%
20	8.087	0.208	0.208	24.86	1.82	24.890	99.88%
30	8.472	0.184	0.184	24.86	1.82	24.894	99.86%
40	8.485	0.22	0.22	24.86	1.82	24.900	99.84%
50	8.448	0.228	0.228	24.8625	1.82	24.907	99.82%
60	8.456	0.229	0.229	24.865	1.82	24.916	99.80%
70	8.449	0.223	0.223	24.8675	1.82	24.927	99.76%
80	8.365	0.223	0.223	24.96	1.82	24.942	99.93%
90	8.308	0.221	0.221	24.96	1.8286	24.964	99.99%
100	8.251	0.216	0.216	24.96	1.8373	24.992	99.87%
120	8.3	0.218	0.218	25.36	1.8953	25.124	99.06%
140	8.601	0.225	0.225	25.56	1.92	25.472	99.65%
160	9.264	0.168	0.168	26.0445	2.1	26.192	99.44%
170	8.79	0.18	0.18	26.4586	2.4766	26.674	99.19%
180	7.68	0.119	0.119	26.978	3.1198	26.947	99.88%
184	16.9	0.07	0.07	27.609	3.2798	27.845	99.15%
188	8.1	0.17	0.17	27.987	3.4399	27.724	99.05%
192	7.97	0.04	0.04	28.275	3.6975	28.574	98.95%
196	8.24	0.11	0.11	28.345	4.0525	28.216	99.54%
200	25.02	0.129	0.129	28.778	4.867	29.086	98.94%
204	22	0.09	0.09	28.83525	5.16	28.815	99.93%

Table 7. *Cont.*

Input Parameters			Actual/Target Values		Predicted Values		Accuracy (in %)
Time Duration	RMS (m/s^2)	Skewness	Total Area (mm^2)	Width (mm)	Total Area (mm^2)	Width (mm)	
208	25.4	0.11	0.11	28.8925	5.4545	30.963	93.31%
212	25.7	0.16	0.16	28.94975	5.7482	29.157	99.29%
216	24.9	0.178	0.178	29.007	6.042	28.649	98.75%
220	13.8	0.12	0.12	28.885	7.0116	28.978	99.68%
224	16	0.16	0.16	28.945	7.0983	28.826	99.59%
229	15.28	0.078	0.078	29.15	7.231	29.602	98.47%
232	19.2	0.26	0.26	29.1725	7.341	30.701	95.02%
239	16.28	0.141	0.141	29.202	7.531	29.257	99.81%
248	19.21	0.151	0.151	29.324	7.761	29.198	99.57%
259	14.86	0.1707	0.1707	29.556	8.631	29.580	99.92%
267.5	8.723	0.14	0.14	29.564	8.987	29.658	99.68%
274.5	9.15	0.041	0.041	31.019	9.362	32.718	94.81%
278.5	9.178	0.115	0.115	33.372	9.761	29.700	87.64%
284.5	9.603	0.014	0.014	36.518	10.401	39.249	93.04%
285	9.114	0.009	0.009	40.157	10.967	39.557	98.48%

It can be observed from Table 7 that the RMS and skewness showed 98.60% accuracy on average. The regression plot and the performance plot for this analysis are shown in Figures 13 and 14, respectively.

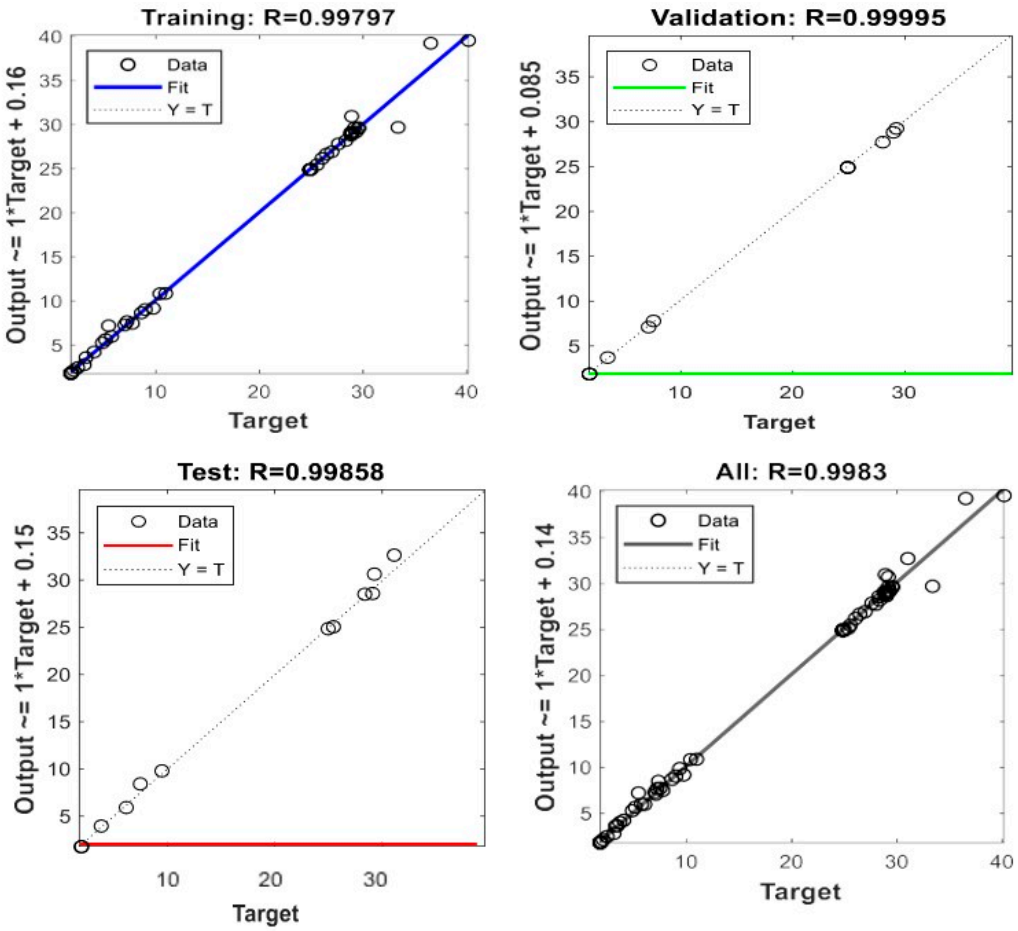

Figure 13. Regression plot for the RMS and skewness.

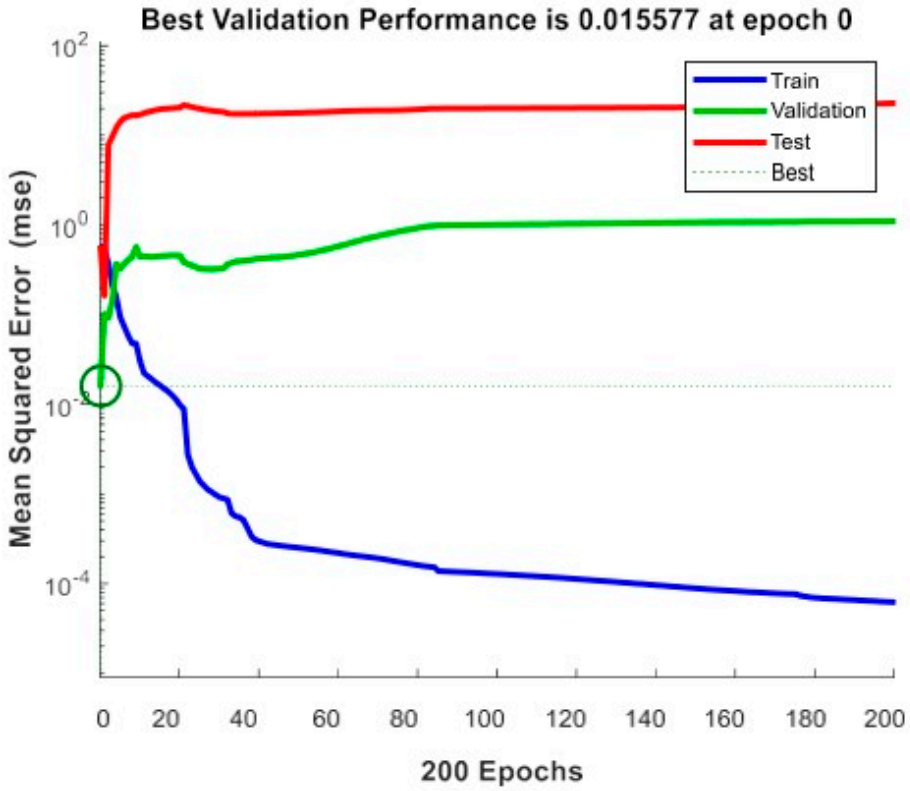

Figure 14. Performance plot for the RMS and skewness.

3.2.4. RMS and Kurtosis

The RMS, kurtosis, and time duration data were used as input parameters in a neural network model, and total area and width were used as goals. This model was then used to create predictions by inputting sample data. Table 8 displays both the expected and actual results.

Table 8. Analyzed data with the RMS and kurtosis as input parameters.

Input Parameters			Actual/Target Values		Predicted Values		Accuracy (in %)
Time Duration	RMS (m/s^2)	Kurtosis	Total Area (mm^2)	Width (mm)	Total Area (mm^2)	Width (mm)	
0	8.347	5.554	5.554	24.86	1.82	24.860	100.00%
10	10.22	6.492	6.492	24.86	1.82	24.860	100.00%
20	8.087	5.527	5.527	24.86	1.82	24.860	100.00%
30	8.472	5.749	5.749	24.86	1.82	24.860	100.00%
40	8.485	5.626	5.626	24.86	1.82	24.860	100.00%
50	8.448	5.913	5.913	24.8625	1.82	24.860	99.99%
60	8.456	5.549	5.549	24.865	1.82	24.860	99.98%
70	8.449	5.618	5.618	24.8675	1.82	24.860	99.97%
80	8.365	5.542	5.542	24.96	1.82	24.860	99.60%
90	8.308	5.603	5.603	24.96	1.8286	24.860	99.60%
100	8.251	5.752	5.752	24.96	1.8373	24.863	99.61%
120	8.3	5.679	5.679	25.36	1.8953	25.170	99.25%
140	8.601	6.147	6.147	25.56	1.92	25.858	98.85%
160	9.264	5.521	5.521	26.0445	2.1	25.981	99.76%
170	8.79	5.728	5.728	26.4586	2.4766	26.438	99.92%
180	7.68	8.537	8.537	26.978	3.1198	26.913	99.76%
184	16.9	7.43	7.43	27.609	3.2798	28.375	97.30%
188	8.1	9.53	9.53	27.987	3.4399	28.002	99.95%
192	7.97	7.67	7.67	28.275	3.6975	29.446	96.02%

Table 8. *Cont.*

Input Parameters			Actual/Target Values		Predicted Values		Accuracy (in %)
Time Duration	RMS (m/s^2)	Kurtosis	Total Area (mm^2)	Width (mm)	Total Area (mm^2)	Width (mm)	
196	8.24	11.6	11.6	28.345	4.0525	27.283	96.11%
200	25.02	7.312	7.312	28.778	4.867	28.935	99.46%
204	22	7.53	7.53	28.83525	5.16	28.846	99.96%
208	25.4	7.15	7.15	28.8925	5.4545	28.966	99.75%
212	25.7	8.63	8.63	28.94975	5.7482	28.864	99.70%
216	24.9	8.017	8.017	29.007	6.042	28.957	99.83%
220	13.8	7.09	7.09	28.885	7.0116	29.168	99.03%
224	16	7.63	7.63	28.945	7.0983	28.889	99.81%
229	15.28	8.1	8.1	29.15	7.231	29.104	99.84%
232	19.2	10.2	10.2	29.1725	7.341	30.250	96.44%
239	16.28	6.48	6.48	29.202	7.531	29.092	99.62%
248	19.21	6.135	6.135	29.324	7.761	29.297	99.91%
259	14.86	6.824	6.824	29.556	8.631	29.299	99.12%
267.5	8.723	4.967	4.967	29.564	8.987	26.822	89.78%
274.5	9.15	6.653	6.653	31.019	9.362	31.452	98.62%
278.5	9.178	6.682	6.682	33.372	9.761	31.975	95.63%
284.5	9.603	7.288	7.288	36.518	10.401	36.292	99.38%
285	9.114	7.954	7.954	40.157	10.967	39.883	99.31%

The RMS and kurtosis showed 98.94% accuracy on average, as shown in Table 8. The regression plot and the performance plot for this analysis are shown in Figures 15 and 16, respectively.

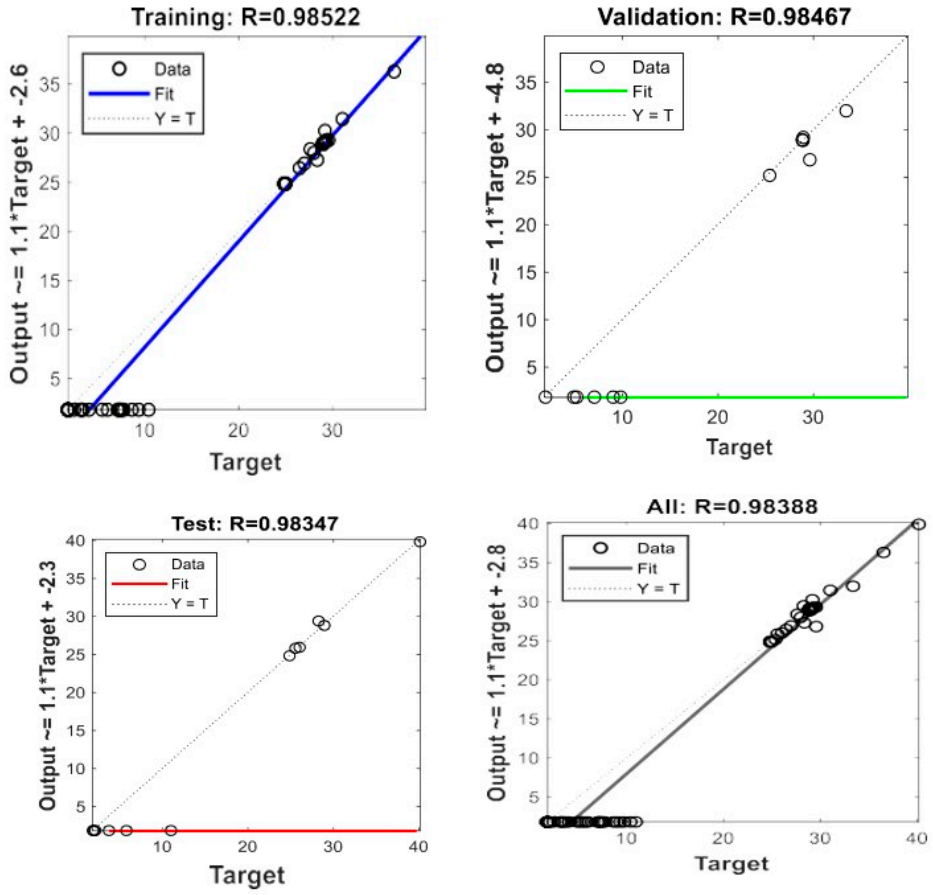

Figure 15. Regression plot for the RMS and kurtosis.

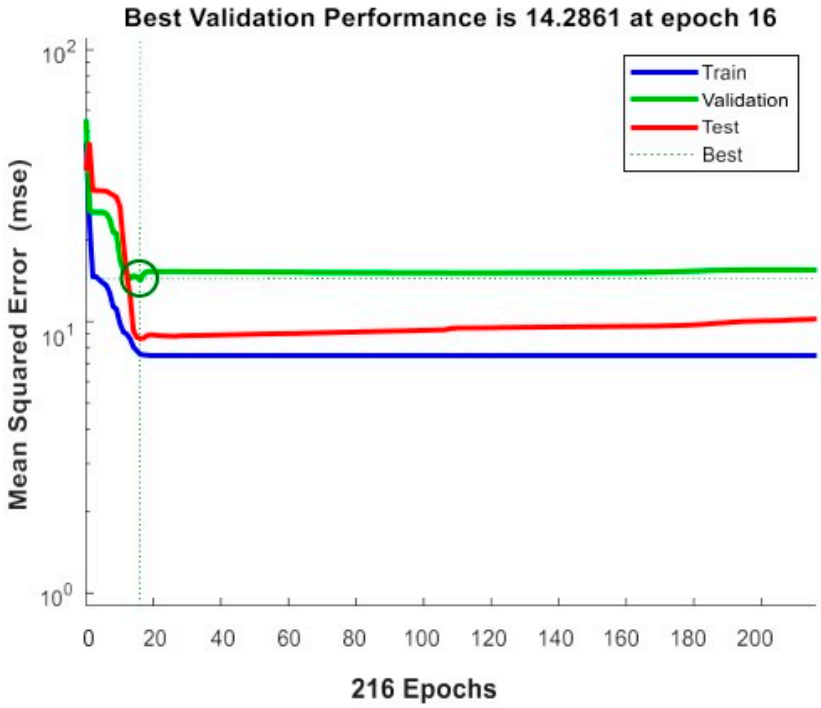

Figure 16. Performance plot for the RMS and kurtosis.

3.2.5. RMS and Shannon Entropy

The RMS, Shannon entropy, and time duration values were used as input parameters in the development of the ANN model, with total area and width as goals. This model was then used to predict outcomes after being fed sample data. Table 9 shows the projected and actual results.

Table 9. Analyzed data with the RMS and Shannon entropy as input parameters.

Input Parameters			Actual/Target Values		Predicted Values		Accuracy (in %)
Time Duration	RMS (m/s^2)	Shannon Entropy (10^7)	Total Area (mm^2)	Width (mm)	Total Area (mm^2)	Width (mm)	
0	8.347	2.42	2.42	24.86	1.82	24.861	100.0%
10	10.22	3.59	3.59	24.86	1.82	24.862	99.99%
20	8.087	2.02	2.02	24.86	1.82	24.861	100.0%
30	8.472	2.27	2.27	24.86	1.82	24.862	99.99%
40	8.485	2.27	2.27	24.86	1.82	24.863	99.99%
50	8.448	2.26	2.26	24.8625	1.82	24.863	100.0%
60	8.456	2.26	2.26	24.865	1.82	24.865	100.0%
70	8.449	2.25	2.25	24.8675	1.82	24.867	100.0%
80	8.365	2.19	2.19	24.96	1.82	24.871	99.64%
90	8.308	2.17	2.17	24.96	1.8286	24.877	99.67%
100	8.251	2.13	2.13	24.96	1.8373	24.891	99.72%
120	8.3	2.16	2.16	25.36	1.8953	24.987	98.51%
140	8.601	2.37	2.37	25.56	1.92	25.438	99.52%
160	9.264	2.8	2.8	26.0445	2.1	26.614	97.86%
170	8.79	2.48	2.48	26.4586	2.4766	27.025	97.90%
180	7.68	2.03	2.03	26.978	3.1198	27.324	98.73%
184	16.9	13.9	13.9	27.609	3.2798	28.520	96.81%
188	8.1	2.07	2.07	27.987	3.4399	27.707	98.99%
192	7.97	1.98	1.98	28.275	3.6975	27.821	98.37%
196	8.24	2.19	2.19	28.345	4.0525	27.875	98.31%
200	25.02	30.7	30.7	28.778	4.867	28.516	99.08%

Table 9. *Cont.*

Input Parameters		Actual/Target Values			Predicted Values		Accuracy (in %)
Time Duration	RMS (m/s^2)	Shannon Entropy (10^7)	Total Area (mm^2)	Width (mm)	Total Area (mm^2)	Width (mm)	
204	22	28	28	28.83525	5.16	28.975	99.52%
208	25.4	20	20	28.8925	5.4545	28.973	99.72%
212	25.7	26	26	28.94975	5.7482	29.006	99.81%
216	24.9	30.5	30.5	29.007	6.042	28.798	99.27%
220	13.8	7.27	7.27	28.885	7.0116	27.910	96.51%
224	16	15.2	15.2	28.945	7.0983	28.516	98.49%
229	15.28	10.2	10.2	29.15	7.231	28.898	99.13%
232	19.2	15.9	15.9	29.1725	7.341	28.486	97.59%
239	16.28	11.7	11.7	29.202	7.531	29.349	99.50%
248	19.21	12.2	12.2	29.324	7.761	29.495	99.42%
259	14.86	9.58	9.58	29.556	8.631	30.125	98.11%
267.5	8.723	2.66	2.66	29.564	8.987	29.749	99.38%
274.5	9.15	3.06	3.06	31.019	9.362	32.180	96.39%
278.5	9.178	13.26	13.26	33.372	9.761	33.544	99.49%
284.5	9.603	3.09	3.09	36.518	10.401	37.427	97.57%
285	9.114	2.74	2.74	40.157	10.967	38.142	94.72%

The RMS and Shannon entropy showed 98.86% accuracy on average, as shown in Table 9. The regression plot and the performance plot for this analysis are shown in Figures 17 and 18, respectively.

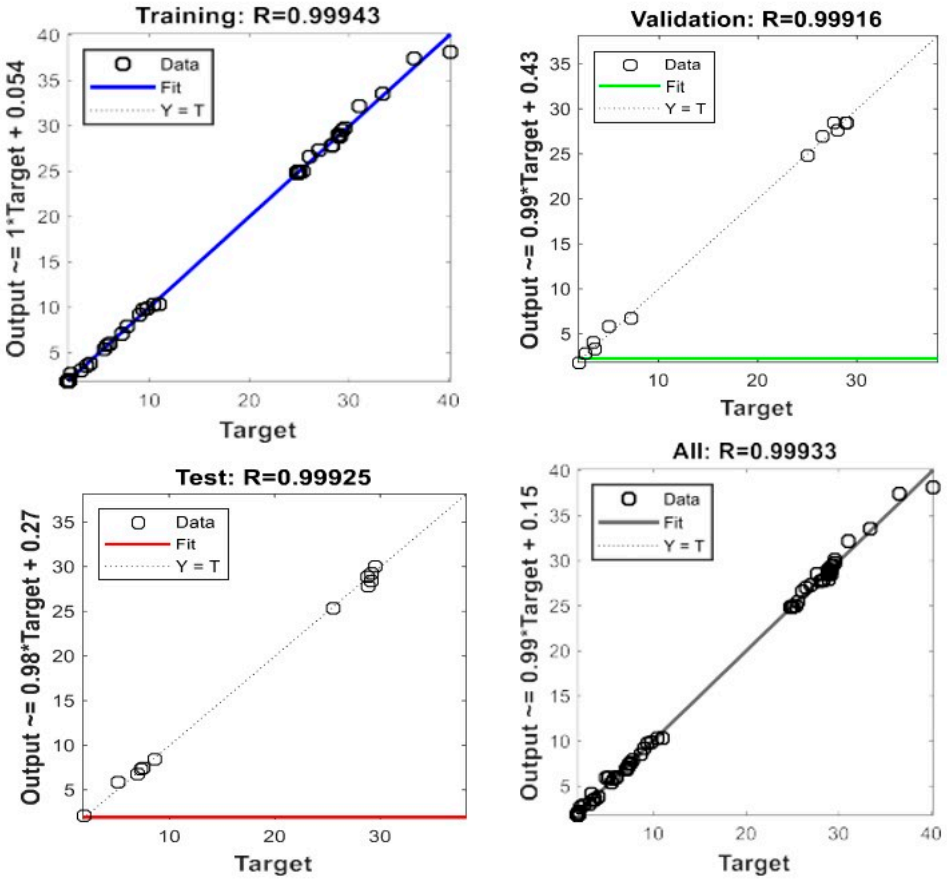

Figure 17. Regression plot for the RMS and Shannon entropy.

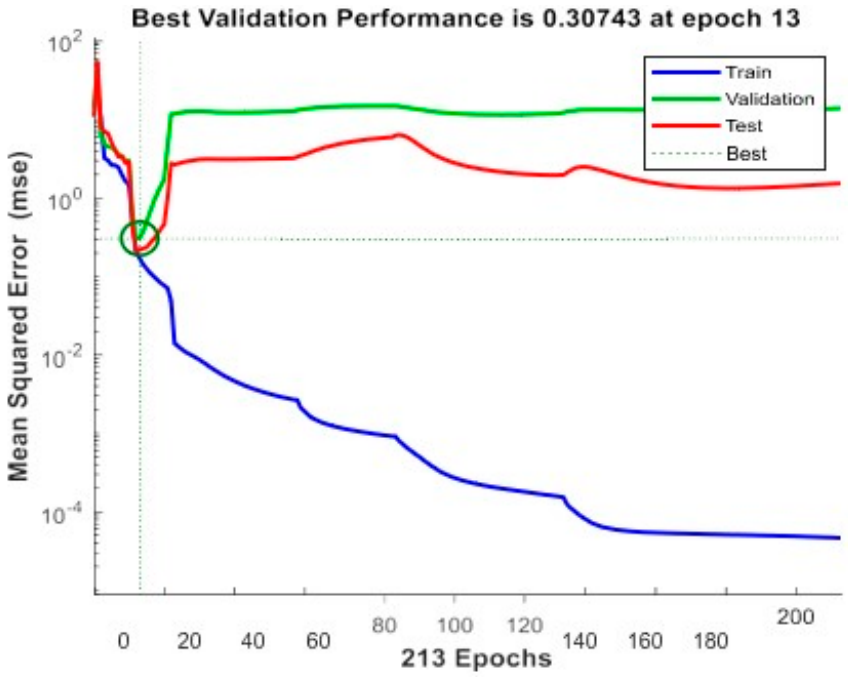

Figure 18. Performance plot for the RMS and Shannon entropy.

3.2.6. Remaining Combinations

The same procedure was followed for the remaining parameters, namely the crest factor, SNR, skewness, kurtosis, and Shannon entropy, with all possible permutations and combinations, and the predicted data, as well as the actual data's accuracy, are shown in Table 10.

Table 10. Accuracy percentages of all the remaining parameters in combinations.

S. No.	Input Parameters	Accuracy (in %)
1	Crest Factor and SNR	96.51%
2	Crest Factor and Skewness	97.64%
3	Crest Factor and Kurtosis	98.87%
4	Crest Factor and Shannon Entropy	97.36%
5	SNR and Skewness	98.17%
6	SNR and Kurtosis	97.81%
7	SNR and Shannon Entropy	96.08%
8	Skewness and Kurtosis	98.41%
9	Skewness and Shannon Entropy	97.45%
10	Kurtosis and Shannon Entropy	99.39%

The accuracy of all possible combinations of the input parameters is shown in Table 10. From Table 10, it is clear that the parameters kurtosis and Shannon entropy show 99.39% accuracy when taken as multi-parameters simultaneously. Furthermore, it is obvious that the multiple-parameter input has slightly higher accuracy than the single-parameter input.

4. Conclusions

After analyzing the findings of our investigation, we can infer that the ANN model performed admirably in predicting data with a better degree of accuracy. While there was some fluctuation for each parameter, our analysis indicates that SNR was discovered to be the most relevant parameter in anticipating data in bearing crack propagation, with an accuracy rate of 99.2% when evaluated as a single parameter. Our investigation was carried out by incorporating the multiple characteristics, and it was discovered that kurtosis and Shannon entropy, when combined, had a 99.39% accuracy rate. This finding suggests that

increasing the number of input parameters can enhance the accuracy of predicting the outcome. In this investigation, the trainlm function was used to predict bearing crack propagation. As a result of these findings, it can be concluded that the ANN model, when combined with numerous input parameters, can provide a more accurate forecast of bearing crack propagation, which has practical applications in the field of machine health monitoring and maintenance. In future, an additional study can be conducted by raising the number of input factors to three or four, which may result in a higher accuracy rate in predicting outputs.

Author Contributions: M.S.: data curation and writing—original draft; D.T.G.: data curation and writing—original draft; S.S.: writing—review and editing; G.V.: data curation, software, writing—original draft, methodology and supervision; S.C.: data curation, software, writing—original draft, and methodology. All authors have read and agreed to the published version of the manuscript.

Funding: No funding has been received for this work.

Data Availability Statement: Data can be made available upon reasonable request.

Conflicts of Interest: The authors declare no conflicts of interest.

References

1. Li, T.; Shi, H.; Bai, X.; Zhang, K.; Bin, G. Experimental analysis and modeling of subsurface cracks with random propagation for ceramic material on rolling contact fatigue. *Eng. Fail. Anal.* **2024**, *155*, 107753. [CrossRef]
2. Zhang, Z.; Chen, Z. A peridynamic model for structural fatigue crack propagation analysis under spectrum loadings. *Int. J. Fatigue* **2024**, *181*, 108129. [CrossRef]
3. Jackson, M.J.; Deng, Z.; Huang, T.; Wei, X.; Huang, H.; Wang, H. Research on Multi-Directional Spalling Evolution Analysis Method for Angular Ball Bearing. *Appl. Sci.* **2024**, *14*, 5072. [CrossRef]
4. Zhang, X.; Wu, D.; Zhang, Y.; Xu, L.; Wang, J.; Han, E.H. Formation Mechanisms and Crack Propagation Behaviors of White Etching Layers and Brown Etching Layers on Raceways of Failure Bearings. *Lubricants* **2024**, *12*, 59. [CrossRef]
5. Bu, J.; Sun, J.; Gao, X.; Su, C.; Du, S. Wear Failure Analysis of Ball Bearings with Artificial Pits for Gas Turbines. *J. Fail. Anal. Prev.* **2024**, *24*, 1365–1375. [CrossRef]
6. Wei, X.; Li, X. Early failure analysis of automobile generator bearing. *Eng. Fail. Anal.* **2024**, *159*, 108124. [CrossRef]
7. Jiang, S.; Du, J.; Wang, S.; Li, C. Simulation and Experimental Study on Crack Propagation in Slewing Bearing Steel. *J. Tribol.* **2024**, *146*, 064301. [CrossRef]
8. Prasad, D.K.; Amarnath, M.; Chelladurai, H.; Santhosh Kumar, K. Assessing the fatigue wear effect on traction coefficient and dynamic performance of roller bearing. *Proc. Inst. Mech. Eng. Part L J. Mater. Des. Appl.* **2023**, *238*, 595–614. [CrossRef]
9. Nasar, R.A.; AL-Shudeifat, M.A. Numerical and experimental analysis on the whirl orbit with inner loop in cracked rotor system. *J. Sound Vib.* **2024**, *584*, 118449. [CrossRef]
10. Liu, Z.; Chang, C.; Hu, H.; Ma, H.; Yuan, K.; Li, X.; Zhao, X.; Peng, Z. Dynamic characteristics of spur gear system with tooth root crack considering gearbox flexibility. *Mech. Syst. Signal Process.* **2024**, *208*, 110966. [CrossRef]
11. Manjunatha, C.M.; Malipatil, S.G.; Nagarajappa, N.; Majila, A.N.; Fernando, D.C.; Bojja, R.; Jagannathan, N.; Manjuprasad, M. Experimental, Analytical, and Computational Studies on the Fatigue Crack Growth Behavior of a Titanium Alloy under Cold-Turbistan Spectrum Loads. *J. Test. Eval.* **2024**, *52*, 931–946. [CrossRef]
12. Mahapatra, S.; Mohanty, A.R. A novel semi-analytical method for fillet foundation deflection calculation in presence of a tooth crack propagating into the rim of a spur gear. *Eng. Fail. Anal.* **2024**, *163*, 108482. [CrossRef]
13. Bovsunovsky, A.; Chernousenko, O. Estimation of Fatigue Crack Growth at Transverse Vibrations of a Steam Turbine Shaft. *J. Vib. Eng. Technol.* **2024**, *12*, 711–718. [CrossRef]
14. Poursaeidi, E.; Javadi Sigaroodi, M.; Aieneravaie, M. Failure investigation of fatigue crack initiation and propagation in compressor blade. *Eng. Fail. Anal.* **2024**, *162*, 108370. [CrossRef]
15. Ansari, A.K.; Kumar, P. Vibration and Acoustics Analyses of Tapered Roller Bearing. *J. Vib. Eng. Technol.* **2024**, *12*, 2467–2484. [CrossRef]
16. Ren, M.; Zhang, Y.; Fan, M.; Xiao, Z. Numerical Simulation and ANN Prediction of Crack Problems within Corrosion Defects. *Materials* **2024**, *17*, 3237. [CrossRef] [PubMed]
17. Xie, M.; Wei, Z.; Zhao, J.; Wang, Y.; Liang, X.; Pei, X. Remaining useful life prediction of pipelines considering the crack coupling effect using genetic algorithm-back propagation neural network. *Thin-Walled Struct.* **2024**, *204*, 112330. [CrossRef]
18. Parsania, A.; Kakavand, E.; Hosseini, S.A.; Parsania, A. Estimation of multiple cracks interaction and its effect on stress intensity factors under mixed load by artificial neural networks. *Theor. Appl. Fract. Mech.* **2024**, *131*, 104340. [CrossRef]
19. Leaman, F.; Vicuña, C.; Clausen, E. Experimental Investigation of Crack Detection in Ring Gears of Wind Turbine Gearboxes Using Acoustic Emissions. *J. Vib. Eng. Technol.* **2024**, *12*, 2111–2128. [CrossRef]

20. Gangwar, M.K.; Sahu, N.K.; Shukla, R.K.; Nayak, C. Machine learning based progressive crack fault monitoring on spur gear using vibration analysis. *Int. J. Veh. Noise Vib.* **2024**, *20*, 89–106. [CrossRef]
21. Hao, M.; Chang, W.; Xu, C. Failure modes determination and load-bearing capacity evaluation of concrete columns under seismic loads by ANNs. *Soft Comput.* **2024**, *28*, 8361–8377. [CrossRef]
22. Chen, Z.; Dai, Y.; Liu, Y. Crack propagation simulation and overload fatigue life prediction via enhanced physics-informed neural networks. *Int. J. Fatigue* **2024**, *186*, 108382. [CrossRef]
23. Shoor, S.; Gopaluni, D.T.; Tamang, W.; Prasad, P.; Singh, H.; Singh, M. Analysis of Crack Dimensions During Crack Propagation Using Neural Network. In *International Conference on Production and Industrial Engineering*; Springer Nature: Singapore, 2024; pp. 209–226. [CrossRef]
24. Min, B.; Zhang, X.; Zhang, C.; Zhang, X. Prediction of bearing capacity of cracked asymmetrical double-arch tunnels using the artificial neural networks. *Eng. Fail. Anal.* **2024**, *156*, 107805. [CrossRef]
25. Li, D.; Nie, J.H.; Wang, H.; Ren, W.X. Loading condition monitoring of high-strength bolt connections based on physics-guided deep learning of acoustic emission data. *Mech. Syst. Signal Process.* **2024**, *206*, 110908. [CrossRef]
26. Liu, M.; Li, H.; Zhou, H.; Zhang, H.; Huang, G. Development of machine learning methods for mechanical problems associated with fibre composite materials: A review. *Compos. Commun.* **2024**, *49*, 101988. [CrossRef]
27. Sahu, D.; Dewangan, R.K.; Matharu, S.P.S. Fault Diagnosis of Rolling Element Bearing with Operationally Developed Defects Using Various Convolutional Neural Networks. *J. Fail. Anal. Prev.* **2024**, *24*, 1310–1323. [CrossRef]
28. Sahu, D.; Dewangan, R.K.; Matharu, S.P.S. An Investigation of Fault Detection Techniques in Rolling Element Bearing. *J. Vib. Eng. Technol.* **2024**, *12*, 5585–5608. [CrossRef]
29. Mutra, R.R.; Srinivas, J.; Reddy, D.M.; Rani, M.N.A.; Yunus, M.A.; Yahya, Z. Dynamic and stability comparison analysis of the high-speed turbocharger rotor system with and without thrust bearing via machine learning schemes. *J. Braz. Soc. Mech. Sci. Eng.* **2024**, *46*, 1–21. [CrossRef]
30. Rivas, A.; Delipei, G.K.; Davis, I.; Bhongale, S.; Yang, J.; Hou, J. A component diagnostic and prognostic framework for pump bearings based on deep learning with data augmentation. *Reliab. Eng. Syst. Saf.* **2024**, *247*, 110121. [CrossRef]
31. Karyofyllas, G.; Giagopoulos, D. Condition monitoring framework for damage identification in CFRP rotating shafts using Model-Driven Machine learning techniques. *Eng. Fail. Anal.* **2024**, *158*, 108052. [CrossRef]
32. Seo, H.W.; Han, J.S. Deep learning approach for predicting crack initiation position and size in a steam turbine blade using frequency response and model order reduction. *J. Mech. Sci. Technol.* **2024**, *38*, 1971–1984. [CrossRef]